TISSUE ENGINEERING: Part B
Volume 16, Number 5, 2010

DOI: 10.1089/ten.teb.2010.0171

Stereolithographic Bone Scaffold Design Parameters: Osteogenic Differentiation and Signal Expression

Kyobum Kim, B.S.,[1] Andrew Yeatts, B.S.,[2] David Dean, Ph.D.,[3] and John P. Fisher, Ph.D.[2]

Scaffold design parameters including porosity, pore size, interconnectivity, and mechanical properties have a significant influence on osteogenic signal expression and differentiation. This review evaluates the influence of each of these parameters and then discusses the ability of stereolithography (SLA) to be used to tailor scaffold design to optimize these parameters. Scaffold porosity and pore size affect osteogenic cell signaling and ultimately *in vivo* bone tissue growth. Alternatively, scaffold interconnectivity has a great influence on *in vivo* bone growth but little work has been done to determine if interconnectivity causes changes in signaling levels. Osteogenic cell signaling could be also influenced by scaffold mechanical properties such as scaffold rigidity and dynamic relationships between the cells and their extracellular matrix. With knowledge of the effects of these parameters on cellular functions, an optimal tissue engineering scaffold can be designed, but a proper technology must exist to produce this design to specification in a repeatable manner. SLA has been shown to be capable of fabricating scaffolds with controlled architecture and micrometer-level resolution. Surgical implantation of these scaffolds is a promising clinical treatment for successful bone regeneration. By applying knowledge of how scaffold parameters influence osteogenic cell signaling to scaffold manufacturing using SLA, tissue engineers may move closer to creating the optimal tissue engineering scaffold.

Introduction

Tissue engineering strategies involving cell/scaffold constructs represent a promising alternative for the treatment of bone injuries. However, the nature and extent of the interactions between cells and the scaffolds are not yet fully understood. Recent research in bone tissue engineering has utilized mesenchymal stem cells (MSCs) for the preparation of cell/scaffold complexes (see Table 1 for a list of definitions). Because of the capability of MSCs to differentiate into multiple tissues, it is of importance to optimize a variety of parameters including chemical, biological, and mechanical cues to induce the osteogenic differentiation of a scaffold-localized cell population. Progenitor MSCs either transplanted to scaffolds before implantation or recruited from surrounding host tissues may differentiate into osteogenic lineages through a series of steps including proliferation, matrix formation, and mineralization.[1] During these stages, a variety of growth factors, cytokines, and hormones are involved and these chemical/biological signals dynamically interact with cell populations to facilitate differentiation cascades. Bone morphogenetic protein-2 (BMP-2),[2–5] fibroblast growth factor,[6,7] transforming growth factor,[8,9] vascular endothelial growth factor,[10–12] and platelet-derived growth factor[7,13] are the major osteogenic growth factors, whereas alkaline phosphatase (ALP) and osteocalcin (OC) are osteogenic differentiation marker proteins. In addition, osteopontin (OP), osteonectin, and bone sialoprotein (BSP) are the important protein components of bone extracellular matrix (ECM).[14,15] Therefore, secreted growth factors from cells may be closely related to the regulation of osteogenic differentiation of a scaffold-localized cell population prior to implantation as well as a recruited cell population from the surrounding host tissues. Enhanced expression of endogenous growth factor genes might facilitate abundant existence of growth factors in the surrounding microenvironment, stimulate the osteogenic differentiation of progenitor cell population, and finally induce bone regeneration. In addition to the upregulation of osteogenic signal expression, the control of dynamic signaling pathways such as Smad, mitogen-activated protein kinase (MAPK),[5,16] Wnt,[17] and the involvement of runt-related transcription factor-2 (Runx2)[18,19] and receptor activator of nuclear factor κB ligand[20] might facilitate a tissue-engineered cell/scaffold construct in bringing about bone tissue regeneration.

The association of many cell/scaffold construction parameters influences osteogenic signal expression. Among those parameters, physical construction factors, specifically

[1]Department of Chemical and Biomolecular Engineering and [2]Fischell Department of Bioengineering, University of Maryland, College Park, Maryland.
[3]Department of Neurological Surgery, Case Western Reserve University, Cleveland, Ohio.

Table 1. Abbreviations and Expansions

3DP	Three-dimensional printing
ALP	Alkaline phosphatase
BMP	Bone morphogenetic protein
BSP	Bone sialoprotein
CAD	Computer-aided design
CARP	Computer-aided rapid prototyping
DEF	Diethyl fumarate
ECM	Extracellular matrix
ERK	Extracellular signal-regulated kinase
FAK	Focal adhesion kinase
GAG	Glycosaminoglycan
HA	Hydroxyapatite
MAPK	Mitogen-activated protein kinase
MSC	Mesenchymal stem cell
NVP	*N*-Vinyl-2-pyrrolodone
OC	Osteocalcin
OP	Osteopontin
PDLLA	Poly(D,L-lactide)
PEG	Poly(ethylene glycol)
PEG–DA	Poly(ethylene glycol)–diacrylate
PEG–DMA	Poly(ethylene glycol)–dimethacrylate
PEO	Poly(ethylene oxide)
PLG	Poly(L-lactic-*co*-glycolide)
PLGA	poly(lactic-*co*-glycolic acid)
PLA	Poly(L-lactide)
PLLA	Poly(L-lactic acid)
PPF	Poly(propylene fumarate)
RhoA	Ras homolog gene family, member A
RGD	Arginine-glycine-aspartic acid
ROCK	Rho-associated, coiled-coil-containing protein kinase 1
Runx2	Runt-related transcription factor-2
SFF	Solid freeform fabrication
SLA	Stereolithography
TCP	Tricalcium phosphate

scaffold design parameters including porosity, pore size, scaffold interconnectivity, and mechanical strength (stiffness), have been shown to influence the osteogenic signal expression and subsequent differentiation of cells seeded on scaffolds both *in vitro* and *in vivo*.[21–24] Further, it has also been demonstrated that these properties might impact the architecture and the amount of *in vivo* bone formation.[25–28] Therefore, the demonstrated importance of these scaffold parameters dictates that an optimal bone tissue engineering scaffold must be achieved for the stimulation of desired signal expression and the induction of osteogenic differentiation of the recruited cell population. Along with the combination of other chemical and biological factors such as the administration of growth factor proteins, the repeated construction of precisely controlled architectures with the optimal design parameters is necessary to achieve an optimal bone tissue engineering scaffold. Stereolithography (SLA) represents a promising advanced scaffold-manufacturing technique to achieve this goal.[29–31] SLA is a rapid prototyping technique that uses photopolymerization to create three-dimensional (3D) scaffolds layer by layer to a design specification that is input via computer.[32–34] This method will enable scaffolds to be reproduced with controlled porosity, pore size, interconnectivity, and mechanical properties, all of which greatly influence osteogenic signaling and differentiation. Therefore, this review will (1) discuss the influence of scaffold construct parameters on *in vitro* osteogenic signaling and *in vivo* bone formation and (2) evaluate SLA as a manufacturing technology to fabricate scaffolds to meet the requirements set forth in the literature.

Structural Parameters to Control Cell Signaling

Effect of porosity and pore size on cell signaling

The ability of a scaffold to enhance osteogenic signal expression and support new bone formation is largely dependent on the pore size and porosity of the scaffold (Table 2). Porosity refers to the overall percentage of void space within a solid, whereas pore size reflects the diameter of individual voids in the scaffold.[35] The importance of scaffold porosity and pore size can be attributed to the native structure of bone, which itself is a porous tissue. Cortical bone is largely a dense structure, but within it exists pores that give an overall porosity of 10%.[36] Porous regions of cortical bone allow for vascularization and cellular infiltration of the structure. Conversely, trabecular bone is a highly porous structure with typical porosity values between 50% and 90%.[36]

Table 2. The Effect of Porosity and Pore Size on Osteogenic Signal Expression and Differentiation

Scaffold materials	*Function and biological improvements*	*Reference*
Collagen–GAG	Pore size affects OC, OP, collagen I, and BSP mRNA expression.	41
	Improved migration in pore sizes larger than 300 μm.	152
Calcium phosphate	Higher pore sizes (280 μm) result in greater osseointegration. Pore size also affects blood vessel formation.	40
	Bone growth is affected more by pore size than porosity. Larger pore size induces greater bone formation.	26
β-TCP	ALP expression affected by size of pores and porosity of scaffolds. Higher mineralization with higher porosity.	21
PLGA	Pore size and porosity affect spatial distribution of new bone formation in cranial defect.	49
Polycaprolactone	Pore sizes between 350 and 800 μm have limited role in bone regeneration after 8 weeks of implantation subcutaneously in mice.	50
	Pore size affects bone formation and type of tissue formed.	27
EH–PEG	Pore size affects BMP-2 expression.	45
HA	Higher ALP expression of human MSCs in smaller pore sizes (200 μm). Higher proliferation in larger pore sizes (500 μm).	23

Porosity and pore size have significant ramifications on the ability of tissue engineering scaffolds to support bone regeneration for several reasons. First, porosity and pore size have been shown to affect cell attachment efficiency, which consequently impacts the cell seeding density, cell distribution, and cell migration.[37,152] These factors have been shown to affect osteogenic differentiation through changes in signaling distances.[38] Moreover, pore size and porosity have a significant effect on the mechanical strength of a scaffold. Sufficient scaffold strength to provide mechanical support to a defect is often required for a hard tissue engineering scaffold such as bone, especially when the bone is load bearing.[39] Further, porosity and pore size affect the ability of the scaffold to promote *in vivo* osteoconduction and vascularization. Integration of native tissue into a scaffold is fostered through growth into interconnected pores, and thus both optimal and minimal pore sizes have been established to support tissue ingrowth.[35,40] Finally, pore size and porosity affect *in vivo* and *in vitro* cell signaling, which in turn affects osteoblastic differentiation of MSCs and the production of ECM proteins.[35,41–45]

Not only must the optimal bone tissue engineering scaffold support the growth and osteogenesis of a seeded cell population, it must also support osteoconduction and vascularization from the surrounding tissue.[46,47] Both osteoconduction and vascularization are influenced by scaffold pore size, porosity, and interconnectivity of pores. In scaffolds with similar porosities ($\sim$50%), it has been established that pore sizes of at least 40 μm are required for minimal bone ingrowth, whereas pore sizes of 100–350 μm are considered optimal.[47,48] In a study analyzing the effect of pore size and porosity on bone healing in a critical-sized rat cranial defect, it was shown that smaller pore sizes (100 μm) induce greater amounts of bone healing than larger pore sizes (500 μm).[49] This study also found a link to porosity, scaffold swelling, and degradation. It may be desirable to have the scaffold size and shape change over time as the scaffold material is resorbed and to have the regenerated bone tissue remodel. In these remodeling cases, the material type and degradation rate should be factored into determining optimal pore volume, pore geometry, interpore wall thickness, and porosity. Scaffolds with larger pore sizes were found to have limited bone growth after about 4 weeks.[49,50] Thus it was hypothesized that smaller pore sizes may enhance continuous host tissue ingrowth. It was also concluded that pore size influences the location of tissue ingrowth, indicating that porosity and pore size should be tailored to different bone types and injury sites, a difficult task with traditional scaffold-manufacturing methods.

In another study, femoral bone scaffolds with pore sizes of 565 μm exhibited higher amounts of bone formation than scaffolds with pore sizes of 300 μm. Within these pore size groups, porosity was also varied from 40% to 50%, but no significant change in bone growth was observed, indicating that porosity may have less of an effect on bone growth than pore size.[26] Despite numerous studies on the topic, there remains disagreement over the significance of pore size on *in vivo* bone formation. In polycaprolactone scaffolds made with pore sizes of 350, 550, and 800 μm, limited differences were observed in the amount of bone growth after 8 weeks.[50] After 4 weeks, the largest pore size group did exhibit greater bone growth, which could indicate that pore size does influence the amount of bone ingrowth, but after 8 weeks, this influence was no longer discernable. It might be possible that more dramatic responses to pore size are only seen at lower pore sizes. For example, it was found that pore sizes of 300 μm induced significantly increased amounts of bone growth after 4 weeks using polycaprolactone scaffolds in a rabbit cranial defect, compared with 100, 200, or 400 μm pore sizes.[27] The discrepancy between these studies could indicate that pore size is not the only variable influencing bone growth. The material type and pore shape as well as the implant size and surrounding tissue vascularization could also influence the effects of pore size on bone ingrowth.

Despite these discrepancies, the influence of pore size and porosity on *in vivo* bone growth has been noted. Pore size has been observed to influence not only the osteoconduction of a scaffold, but also the vascularization, which is crucial to successful bone formation. In a study utilizing calcium phosphate ceramics, pore sizes of 140–280 μm exhibited faster vessel formation than pores of 40–140 μm. Also larger pore sizes had significantly higher capillary density than small pore sizes. The volume of new bone correlated with these results as the largest pore size group (210–280 μm) had the most new bone growth.[40] Rapid vascularization is important for bone tissue growth in an implanted scaffold as cells on the interior portions of the scaffolds will not survive without a blood and nutrient supply. Oxygen and nutrient transfer distances are limited to $\sim$200 μm, making vascularization a concern even in smaller scaffolds.[51] The degree of vascularization in a bone tissue engineering scaffold also influences the mechanism by which bone formation occurs.[40,52] Hydroxyapatite (HA) scaffolds with pore sizes of 90–120 μm were shown to support bone formation by a process of endochondral ossification where MSCs proliferate on the scaffold and begin to form cartilage tissue.[53] The cartilage then begins to become vascularized and is resorbed by phagocytic cells. MSCs migrate to the site, differentiate into osteoblasts, and begin to form bone. This process can lead to highly organized bone structures observed in long bones.[36] Scaffolds with pore sizes of 350 μm were observed to form bone through intramembranous ossification where MSCs initially migrate in with vascularization and form new bone directly without any cartilage formation.[53] This type of bone formation is typical in the cranium and other flat bones. Pore size can influence the method of bone formation as it affects the degree of vascularization, which in turn affects the oxygen present in the tissue and ultimately whether chondrogenesis or osteogenesis occurs. Therefore, the effect of pore size on the mechanism that results in bone formation underscores the importance of precise control over the pore size and porosity of the scaffold and pore architecture may need to be tailored to specific bones for effective tissue engineering.

In addition to *in vivo* bone growth, it has also been shown that *in vitro* cell growth and differentiation on scaffolds are greatly affected by pore size and porosity. *In vivo* porosity and pore size mainly influence bone growth by influencing the native tissue that invades the scaffold, whereas *in vitro* studies have emphasized the influence of pore size and porosity on the migration, proliferation, differentiation, and signaling of cells within a scaffold.[35] For instance, Mygind *et al.* have shown the effect of pore size on the expression of a series of osteogenic signals.[23] Human MSCs cultured on

coralline HA scaffolds exhibited lower proliferation rate and higher degree of differentiation as shown by increased ALP, OC, and BMP-2 mRNA expression on scaffolds with a smaller pore size (200 μm) as opposed to a larger pore size (500 μm). The enhancement of osteogenic differentiation and a lower proliferation rate may both be explained by the difference in surface area and transport efficiency resulting from the change in pore size. It might be suggested that a scaffold geometry with smaller pore size resulted in increasing tortuosity, thereby decreasing transport efficiency of soluble factors in the aqueous surrounding environments and limiting the cell infiltration. Subsequently, decreased proliferation might be observed because of changes in signaling distances by varying the pore geometry that induces a higher level of differentiation. Another study has also shown that pore size and porosity influence expression levels of osteogenic signals. In collagen–glycosaminoglycan (GAG) scaffolds, greater expression of OC and type I collagen in MSCs after 21 days of culture was observed in scaffolds with pore sizes of 151 μm when compared with 96 μm.[41] Moreover, pore size has also been shown to influence the differentiation of human MSCs on β-tricalcium phosphate (β-TCP) scaffolds with varying porosities (25%–75%) and pore sizes (10–600 μm, respectively).[21] In this research, no significant difference was observed in the *in vitro* osteogenic differentiation between the groups. However, when the samples were implanted into skin folds of mice, a significantly higher amount of osteoblastic differentiation was observed as shown by ALP production in scaffold constructs with 65% and 75% porosities, with the highest amount observed in the 65% group. This study indicates that porosity may not be the sole influence of osteogenic differentiation and that differences in signal expression might be observed relating to pore size *in vivo* even without bone ingrowth from surrounding tissues.[21] Using an EH-PEG hydrogel fabricated from poly(ethylene glycol)–diacrylate (PEG–DA) and 5-ethyl-5-(hydroxymethyl)-β,β-dimethyl-1,3-dioxane-2-ethanol diacrylate (EHD), the effect of pore size and porosity on the BMP-2 signaling of human MSCs was investigated in scaffolds with pore sizes of 100 and 250 μm.[45] In this study, BMP-2 signaling was upregulated in the scaffolds with 250 μm pore size when compared with those with 100 μm pore size with the same porosity on days 4, 8, and 12. This indicates that pore size has an effect on BMP-2 signal expression. Further, 50–70-fold increases in BMP-2 expression were observed in 3D porous gels when compared with 2D monolayer culture, highlighting the effect of 3D architecture on signal expression. It was hypothesized that this effect resulted from a concentration of signaling molecules within the hydrogel, enhancing autocrine and paracrine cell signaling.

Scaffold porosity and pore size can influence *in vitro* growth and differentiation of a seeded MSC population, although these effects are often less-pronounced ways than *in vivo* bone growth. Although much research has been done in this area, further studies are necessary to determine the optimal pore size for *in vitro* bone growth and to fully elucidate the effect of pore size and porosity on cell signaling. For the future of bone tissue engineering, highly controlled and characterized scaffolds must be created to not only further evaluate the influence of porosity and pore size, but also to create scaffolds with reliable geometries to ensure predictable clinical use.

Scaffold interconnectivity

Another important characteristic of scaffold architecture is the degree of interconnectivity between the pores of a scaffold. Scaffolds that feature a highly interconnected architecture allow for enhanced communication between cells at different areas within a scaffold and promote tissue ingrowth (Table 3). Scaffold interconnectivity has been shown to have a limited direct effect on MSC signaling and differentiation, but a profound effect on the morphology of bone formed within a scaffold.[54–56] When human MSCs were seeded on silk constructs, no significant differences were observed in ALP expression and calcium deposition after 4 weeks of culture between scaffolds with different levels of interconnectivity.[54] However, significant differences were observed in the degree of cellular ingrowth in the scaffolds. It was observed that growth into scaffolds with low interconnectivity was confined to surface pores, whereas highly interconnected scaffolds featured homogenous mineralization and a network of

Table 3. The Effect of Interconnectivity on Osteogenic Signal Expression and Differentiation

Scaffold materials	*Function and biological improvements*	*Reference*
PLG	Faster colonization in scaffolds with large scaffold interconnectivity. No change observed in gene expression levels of vinculin, β-actin, OC, or OP with changes in scaffold interconnectivities.	57
Silk fibroin	Interconnectivity influences morphology of *in vitro* bone growth of human MSCs but not ALP protein expression.	54
HA	*In vitro* cell penetration enhanced by large interconnected channels, established minimum channel size of 80 μm for cell penetration.	55
	Enhancement of bone ingrowth observed in channels over 100 μm. Micro-computed tomography used to assess bone growth.	60, 61
	Scaffolds manufactured using SFF. Geometry of channels influence *in vivo* bone growth.	24
	Scaffolds formed from mold using SLA. Individual channels should be interconnected for increased bone growth.	25
HA/β-TCP	Osteoblasts could penetrate channels as small as 20 μm but could not form bone until channel diameter reached 50 μm. Also, changes were observed with material type.	59
Titanium	Length and size of pore connection to surface of scaffold influenced the amount of bone ingrowth.	62
PLGA/β-TCP	Scaffolds manufactured using SFF. Macroscopic channels guide bone growth and dictate tissue type produced.	28

bone-like tissue. In another study using poly(L-lactide-*co*-glycolide), levels of vinculin, β-actin, OC, and OP of human MG63 cells were similar for scaffolds with varying interconnectivities.[57] Greater penetration depth was observed in scaffolds with larger pore sizes and higher interconnectivity, although these differences diminished after 15 days. This study suggested that increasing pore size and interconnectivity yielded faster colonization of cells and that degree of interconnectivity should be tailored to bone cells as connective tissues may infiltrate more quickly into smaller connections, resulting in inhibition of bone tissue infiltration. Scaffold interconnectivity may also affect bone formation and osteogenic signal expression by affecting the degree of nutrient diffusion into a scaffold.[58] As previously described, bone nutrient and oxygen transfer are a concern in any 3D construct.

Degree of interconnectivity is not the sole factor influencing bone ingrowth, as the diameter of channels connecting pores has also been shown to influence cell penetration. In a study to investigate the effect of channel diameter on cell penetration *in vitro* using HA scaffolds and human osteosarcoma cells, it was found that larger channel diameter resulted in both increasing cell coverage and deeper penetration into the center of the scaffold.[55] Further, it was also found that there was a minimum level of channel diameter required for cell penetration (82 μm).[55] Similarly, in another study, human osteoblasts were shown to penetrate channels over 20 μm, but a pore size of 50 μm was required to support new bone formation through the channels.[59] This study indicated that the minimum channel size might vary with the dimension and material of a scaffold, as interconnectivity fosters not only cell infiltration but also vascularization and nutrient transfer, highlighting the need for controlled scaffold interconnectivity.

Scaffold degradation impacts ingrowth as well, and therefore, this factor needs to be considered in tandem with interconnectivity for optimal tissue formation. Because of the complexity of the network inside of a scaffold, pore interconnectivity can be difficult to assess, but the use of micro-computed tomography (CT) to quantify pore interconnectivity allows for a more precise definition and better assessment of scaffold characteristics.[60–62] Precise scaffold interconnectivity is difficult to create using traditional scaffold fabrication techniques, and thus advanced scaffold manufacturing may be necessary to achieve repeatable interconnectivity. Advanced manufacturing techniques include scaffolds made through the use of rapid prototyping, which is also known as solid freeform fabrication (SFF) and additive manufacturing. In one example of enhanced scaffold interconnectivity using SFF, poly(lactic-*co*-glycolic acid) (PLGA)-β-TCP scaffolds were fabricated using the commercially available TheriForm™ 3D printing process (3DP).[28] To test the effect of interconnected continuous channels on bone ingrowth, scaffolds were manufactured with either macroscopic channels or a microscopic porosity gradient. Using a rabbit cranial defect model, histomorphometric analysis after 8 weeks of implantation demonstrated that scaffolds with macroscopic channels had a higher new bone area than both the scaffolds without channels or the defect without any scaffold. These results indicated that *in vivo* bone formation was guided down the channels of the scaffold. Further, the porosity gradient of the scaffold was shown to dictate the type of tissue that was produced, as only soft tissue was produced outside the radial channels of the scaffold. This suggests that the precise architecture of a scaffold can be used to guide tissue growth.[28]

By manipulating the porosity and interconnectivity, the rate of bone tissue regeneration may be enhanced. On the basis of an *in vivo* study utilizing HA scaffolds fabricated by 3DP and rabbit cranial defects, it was suggested that the direction and the extent of void space in the scaffold might influence new bone formation.[24] Histological evaluation indicated that the channels direct the growth of new bone, as radial channels penetrating from the sides of the scaffold were shown to successfully guide bone from the surrounding tissue and axial channels extending inward from the bottom of the scaffold directed the migrating cells into the center of the scaffold. This study provided further evidence that *in vivo* bone growth could be influenced by the scaffold architecture and interconnectivity. Moreover, a similar result with respect to controlling *in vivo* bone growth through scaffold architecture and interconnectivity was observed in SLA-fabricated HA scaffolds.[63] To investigate the *in vivo* performance of channel directions, scaffolds with orthogonal or radial channels were implanted into porcine mandibles. The scaffold architecture was shown to influence the amount of regenerated bone, as the orthogonal scaffolds exhibited larger bone growth area than scaffolds with radially oriented channels. The lack of interconnectivity between the individual channels might explain the reduced bone growth in radially channeled scaffolds. In addition, it appears that the architecture in the porous regime might influence bone geometry, as bone formation was integrated throughout the orthogonal HA scaffolds, whereas the bone in the radial scaffolds formed an intact piece in the center of the scaffold.[63] These studies may validate the use of scaffold interconnectivity and architecture to guide bone growth and enhance *in vivo* bone tissue regeneration. Additional work using scaffolds with highly characterized and controlled interconnectivity should be completed to further elucidate the connection between the two.

Mechanical stiffness and mechanosensing

Dynamic cell–ECM interaction may regulate initial cell attachment, proliferation, differentiation, and osteogenic and chondrogenic signal expressions. Among a variety of scaffold design parameters, including pore geometry and interconnectivity, substrate stiffness (rigidity) is another critical factor governing cellular behavior in terms of mechanotransduction and cell–matrix interaction. There have been many studies of the effect of substrate stiffness on the cellular behaviors in several tissue types including bone,[64] the central nervous system,[65] the cornea,[66] and kidney epithelial cells.[67] Different tissues present characteristic elasticities, ranging from ~1 kPa in the brain to 100 kPa in collagenous bone. The specific type of cells in each tissue favored to differentiate into different lineages depending on the scaffold's mechanical stiffness.[68] Recent studies have revealed that the substrate stiffness is directly related to the specific differentiation cascades that an MSC population undergoes. Therefore, the mechanical properties of a scaffold could be another critical parameter in designing the optimal 3D scaffold for bone tissue engineering (Table 4).

Table 4. The Effect of Mechanical Stiffness on Osteogenic Signal Expression and Differentiation

Scaffold materials	*Function and biological improvements*	*Reference*
Polyacrylamide gel	Tunable stiffness by varying the amount of crosslinker. Proliferation of MC3T3-E1 cells, random motility speed, FAK activity, and mineralization could be affected by substrate stiffness.	22
	Controlling the ECM stiffness and incorporation of ECM protein may regulate the human MSC differentiation into osteogenic and myogenic lineages.	71
PEG hydrogel	ECM rigidity may regulate ALP, OC, and BSP expression via MAPK activation. Sequential activation of FAK, RhoA/ROCK, and ERK/MAPK by controlling ECM rigidity.	16, 69
2D polystyrene	Stiffness-dependent osteogenic signal expression and mineralization in embryonic stem cells.	70
PEG–fibrinogen hydrogel	Modulation of cytoskeletal assembly of smooth muscle cells by varying the stiffness. Synergetic effect of stiffness and RhoA activation on cytoskeletal contractility.	73
Polyester copolymer	Controllable crosslinking density by varying the composition of copolymer and the type of initiator.	75
Gelatin/β-TCP	β-TCP amount may affect compressive modulus, ALP activity, and OC expression.	77
PLGA/chitosan	Cell adhesion and calcium deposition could be affected by PLGA/chitosan ratio.	78
Matrigel with microfabricated SU-8	mRNA expression of osteogenic signals of human MSCs may be influenced by embedded SU-8.	80
Collagen–GAG	Tunable compressive modulus of scaffolds through dehydrothermal crosslinking process.	88
Denser collagen matrix	Denser collagen matrix exhibited increased expression of ALP and BSP.	87

It has been investigated that the responses of osteoblast cell populations could be affected by intrinsic ECM mechanical properties.[22] In this study, polyacrylamide hydrogels were functionalized with type I collagen and fabricated with various Young's moduli depending on the amount of crosslinker, *N*,*N*′-methylene-bis-acrylamide. The substrate stiffness ranged from 11.78 to 38.89 kPa by varying the amount of crosslinker from 0.1% to 0.3%. When the collagen density was low, the proliferation of MC3T3-E1 cells was higher on a rigid polystyrene substrate than on the softest gel and the random motility speed of cell migration was also faster on polystyrene than on a soft substrate. The result suggested that the modification of ECM mechanical properties might influence the contractility in the actin cytoskeleton, and immature focal contact and cytoskeleton development in the softest gel could verify this rationale. Moreover, both focal adhesion kinase (FAK) activity measured by detecting phosphorylated Y397-FAK and mineralization determined by qualitative Von Kossa staining demonstrated that signaling mechanisms of cell–ECM and osteogenic phenotypic differentiation were modulated by the ECM stiffness. A similar study has shown that cellular responses to scaffold mechanical properties may regulate the osteogenic differentiation by modulating the MAPK and the extracellular signal regulated kinase (ERK) activity.[16,69] The results demonstrated that osteogenic differentiation of MC3T3-E1 cells cultured on mechanically tunable PEG hydrogels could be regulated by substrate rigidity. In particular, phosphorylation of p44/42 MAPK was enhanced as the rigidity increased and this regulation of MAPK activity might be related with upregulation of ALP activity as well as the OC and BSP gene expression levels.[69] In addition, it was also found that altered ECM mechanics activates the FAK activity through integrin-mediated signal transduction.[16] Enhanced FAK activity stimulates Ras homolog gene family, member A/Rho-associated, coiled-coil-containing protein kinase 1 activity, and this signal subsequently stimulates the ERK/MAPK. Finally, Runx2 in a nucleus is activated and osteogenic gene expression including OC, BSP, and ALP may be upregulated. This sequential signal transduction triggered by matrix stiffness would ultimately lead to osteogenic differentiation of cells on the substrate material.

Further, stiffness-dependent osteogenic signal expression was also observed in embryonic stem cells.[70] The expression levels of osteogenic marker genes including Runx2 and OP were dependent on the surface Young's modulus of collagen-coated polydimethylsiloxane substrates. Upregulation of the primitive streak and mesoderm precursors including forkhead transcription factor, Brachyury, Mix 1 homebox-like 1, cadherin-2, and eomesodermin homolog (Eomes) was observed. In addition, mineralization assessed by alizarin red S was also positively correlated with the stiffness substrates from 0.041 to 2.7 MPa.

However, downstream differentiation of cells and changes in phenotype do not solely depend on mechanical cues that the cell receives from a scaffold, but also on a combination of factors of the cell's physical, chemical, and biological ECM properties. Rowlands *et al.* demonstrated that varying substrate stiffness could regulate the human MSC differentiation into either osteogenic or myogenic lineages.[71] In this study, polyacrylamide gels coated with ECM proteins including collagen I, collagen IV, laminin, and fibronectin were investigated. Physiologically relevant stiffness (0.7–80 kPa) was obtained by crosslinker fraction and cultured MSCs exhibited different levels of Runx2 and myogenic differentiation-1 expressions, which represented osteogenic and myogenic

transcription factors, respectively. Specifically, the substrate model with an 80 kPa of modulus and a collagen type I coating showed the highest expression level of both transcription factors. This might suggest that mechano-transduction is related to both scaffold stiffness and adhesive ligand presentation on the ECM. This observation was also made in 2D gel systems as the osteoblastic function of cells was altered by changing type I collagen density[22] and other ECM protein coatings.[72]

In addition to osteoblastic cells, smooth muscle cells have been observed to exhibit similar behavior on substrates with varying stiffness.[73] In this study, 3D crosslinked PEG–fibrinogen hydrogel encapsulating cells exhibited 4.48–5.41 kPa of compressive modulus. This range of stiffness in the 3D environment appeared to modulate cytoskeletal assembly. From this research, it may be suggested that small changes in the mechanical stiffness of scaffold materials may alter the biological functions and phenotype of transplanted cell populations. Another fundamental finding of this study was that a synergetic effect between substrate stiffness and Ras homolog gene family, member A activation appears to be critical to the regulation of cytoskeletal contractility. As shown in another study, cell shape and morphology and the subsequent changes in contractility may regulate the downstream cell functions.[74]

Crosslinking density. Mechanical properties of 3D polymeric scaffolds such as compressive modulus could be controlled by changing the crosslinking density during fabrication or by varying the ratio of composite filler materials. For instance, crosslinking density of polyester scaffolds fabricated with D,L-lactide, ε-caprolactone, and trimethylene carbonate could be controlled by varying the composition of copolymers and the type of initiator, and therefore, the degradation ratio, as well as the compressive modulus, of scaffolds could also be varied.[75] Similar to the modulation of crosslinking density of 2D gel systems described previously, the amount (or the ratio) of crosslinker within polymeric matrices could be used to control the modulus of porous scaffolds. In addition, a study of poly(propylene fumarate) (PPF) photocrosslinking characteristics also demonstrated that mechanical properties could be controlled by fabrication parameters including the molecular weight of the PPF polymer, photoinitiator content, and the amount of the present diester precursor, diethyl fumarate (DEF).[76] In this study, sol fraction, swelling degree, elastic modulus, and fracture strength were examined based on the factorial design of three fabrication factors. In particular, the results indicated that varying these factors could control crosslinking and compressive mechanical properties. Moreover, this study exhibited the feasibility of PPF/DEF mixture for the reduction of viscosity to use PPF as an SLA resin material and the suitability of this polymer network with compressive strength for trabecular bone replacement. Thus, controlling the crosslinking density of the polymer network could change the mechanical stiffness of a scaffold, and this controllability could be utilized in SLA rendering.

Filler incorporation. Another method to control the stiffness of 3D scaffolds is incorporation of fillers into polymeric scaffold resins. For example, the gelatin scaffold incorporated with β-TCP also exhibited varying compressive modulus from 0.27 MPa (no β-TCP incorporation) to 4.97 MPa (90 wt% of β-TCP) depending on the amount of β-TCP particles.[77] The highest ALP activity and OC content of rat MSCs were observed in 50 wt% of β-TCP, and it could be concluded that the composition ratio of composites might change the compressive modulus of a 3D scaffold and the expression of osteogenic marker proteins might be related to this ratio with the threshold up to 50 wt%. Similarly, when chitosan was incorporated into PLGA polymeric scaffolds, increasing the chitosan/PLGA ratio resulted in increasing adhesion efficiency of seeded rat bone marrow stromal cells as well as increased calcium deposition, which indicated that the majority of cell population underwent osteogenic differentiation.[78] In addition to mineral particle incorporation, microfabricated SU-8 microrods ($15\times15\times100\,\mu m$) in a 3D commercialized Matrigel might result in increasing stiffness of the 3D matrix and influence the fibroblast attachment pattern.[79] Given changes in morphology and cytoskeletal architecture, the mechano-transduction mechanism might be altered and the signal expression profiles of human MSCs cultured in this matrix system exhibited upregulation of actin related protein (ACTR) and phosphatase and actin regulator (PHACTR) as well as downregulation of collagen I and BMP-6 expression.[80]

However, incorporation of filler material into polymeric resin may alter not only the stiffness of composites but also the surface characteristics including topology, roughness, passive adsorption of soluble contents, and the overall scaffold's chemical composition.[81,82] In addition to changing the mechanical stiffness by incorporating filler material into polymeric scaffolds, controlling of physicochemical surface properties may facilitate the interaction of hosted cell population and a scaffold. Inorganic particle incorporation of β-TCP or HA provides a biochemical environment that closely mimics native bone, and this might result in dynamic interaction of Ca^{2+} ions with the seeded cells[83] as well as *in vivo* tissue regeneration.[8,84]

Collagen. As collagen is an important ECM protein found in the native bone, its structural properties have been researched in bone tissue engineering to lead to skeletal tissue regeneration strategies.[85] Therefore, the proper production and crosslinking of collagen in the ECM environment could lead to osteogenic differentiation of recruited cells.[86] The stiffness of the collagen matrix has also shown that it functionally stimulates implanted cell populations.[87,88] The compressive modulus of collagen–GAG scaffolds could be controlled by varying the collagen amount as well as by altering the dehydrothermal crosslinking process.[88] Specifically, the 1% collagen–GAG scaffolds that were treated with a higher crosslinking temperature exhibited increased cell numbers and metabolic activity up to 7 days after culture. Another study using a dense collagen matrix showed upregulation of osteogenic signal expression in primary mouse calvarial osteoblasts.[87] Osteogenic differentiation of cells in the matrix were verified through the observation of increased expressions of ALP and BSP in the first 7 days of culture in osteogenic supplemented media, which was compared with culture on a 2D plastic surface.

It might not be concluded that the stiffness or compressive modulus of scaffolds directly govern the specific signal expressions that would bring about bone tissue differentiation

cascades. The complex signal transduction involved in osteogenesis is dynamically related to cell–cell and cell–ECM interaction as well as intracellular mechanisms. However, the combinational approaches of controllable mechanical strength and other stimulatory factors such as ECM protein incorporation and topological changes of the substrate surface may allow manipulation of the level of expressions of osteogenic signals and, eventually, differentiation. Given this concept, SLA can also be applied to create the tunable stiffness or other mechanical characteristics in 3D bone tissue engineering scaffolds.

Computer-Aided Rapid Prototyping

Stem cell-based tissue engineering approaches may benefit from optimization of scaffold design parameters with the aid of chemical and biological stimuli in order for the stages of cell proliferation and osteogenic differentiation during *in vitro*, as well as *in vivo* osteogenesis. As discussed earlier, the architectural parameters, including porosity, pore size, interconnected channel geometry, chemical properties such as crosslinking density, and mechanical cues such as stiffness, are important factors for bone scaffold fabrication. These factors might stimulate cell responses including the signal expressions facilitating cell differentiation. Because of the variations observed when altering these factors, it is necessary to first define the optimal values of parameters to enhance cellular responses. Then, accurate fabrication and continuous production of the scaffolds with the optimal architectural, chemical, and mechanical parameters could justify extending the use of bone tissue engineering to clinical regenerative medicine with improved levels of bone regeneration at implanted sites. Therefore, computer-aided rapid prototyping (CARP) is considered to meet these criteria with sufficient control in scaffold preparation to provide improved tissue regeneration, proper vascularization after implantation, and sufficient tissue integration with scaffold degradation. The CARP process produces scaffolds layer by layer through SFF with design parameters inputted from computer-aided design (CAD) software. Precise control of these parameters is the most significant advantage of CARP; thus, when designing a scaffold's inner architecture, the ability of the design to influence the forming bone geometry should be considered in addition to its effects on osteogenesis.[89]

Another advantage of CARP for the fabrication of scaffolds is its feasibility of patient- and defect-specific design of bone implants.[90,91] SFF includes several types of commercially or readily available techniques that have been utilized to produce directly implantable tissue-engineered (i.e., resorptive) implants.[29,92] 3D printing (3DP™; Therics, Inc., Princeton, NJ) injects a liquid binder, which may contain cells and/or growth factors, into a powder.[93] Fused deposition modeling (Stratasys, Inc., Eden Prairie, MN) uses an inkjet to extrude material that is heated just above melting temperature.[94] 3D plotting is another heat-based extrusion technique.[95] In selective laser sintering (3D Systems, Rock Hill, SC), a laser is used to sinter powder, layer by layer, into a plastic part.[96] Selective laser melting (MTT, Staffordshire, UK) uses a laser to sinter metal powders.[97] Solidscape (Merrimack, NH) devices print an implant shape in wax that can then be replaced with resorbable materials.[98] Soft lithography (Nanoterra, Cambridge, MA)[99] and electrospinning[100] are technologies that can produce very high-resolution surface features, such as roughness on a scale relevant to cells.

Stereolithography

One of the most researched SFF methods is SLA (3D Systems), which utilizes a laser to crosslink photopolymerizable polymers and fabricate 3D parts by vertical layering.[101] Figure 1 shows a schematic of SLA fabrication. The modeling of pore structure in porous tissue-engineered scaffolds was highlighted elsewhere.[29] Therefore, SLA is a useful strategy to fabricate precisely designed scaffolds with defect site-specific external shape based on a patient's 3D CT scan, as well as parameters such as pore size, porosity, interconnectivity, and mechanical stiffness optimized to influence osteogenic signal expression and differentiation (Table 5).

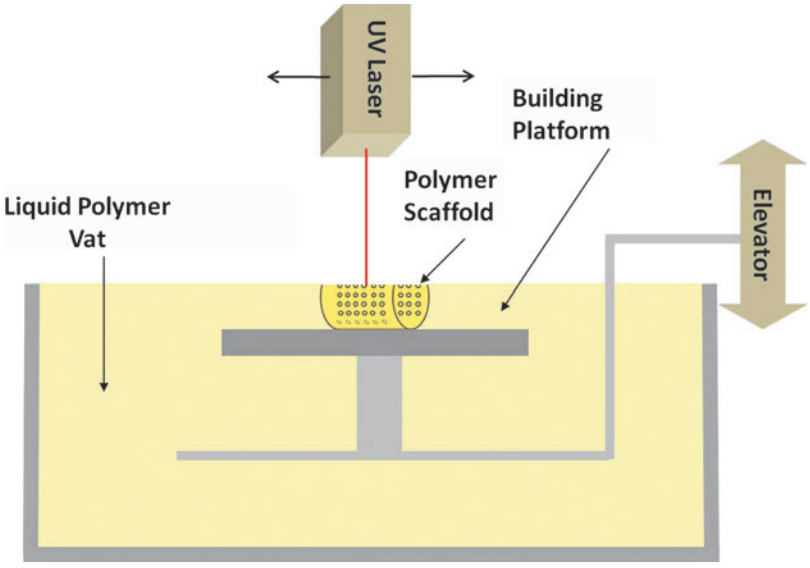

FIG. 1. A schematic of the stereolithography (SLA) process. A laser crosslinks the liquid polymer at the surface of the polymer vat, according to specifications inputted in the computer, by moving in the *X* and *Y* directions. Following completion of a layer, the elevator lowers the completed scaffold one layer in the *Z* direction and the process repeats.

Table 5. Recent Development of Stereolithography in Bone Tissue Engineering Research

Scaffold materials	*Function and biological improvements*	*Reference*
PPF	Controllable mechanical properties and crosslinking characteristics of PPF/DEF/photoinitiator mixture.	76
	Initial trial of PPF resin by using a commercialized SLA machine (3D Systems, Rock Hill, SC).	101
	Surface modification after scaffold fabrication.	102
	Fabrication of controlled architecture with 250–260 μm pore size and 132–143 μm line width.	103
	Utilization of PPF with low number average molecular weight (<800 Da).	102, 106
PDLLA/NVP	Fumaric acid monoethyl ester-functionalized PDLLA/NVP could be used with SLA resin material and aid of accelerator/photoinitiator to form 240–350 μm pore sizes in gyroid structures.	107
PDLLA	Formed scaffold with 73 vol% porosity and 170–240 μm pore size in gyroid structures.	108
PLLA	Used a negative mold fabricated by SLA. Upregulation of OC and BSP mRNA expression in nanofibrous scaffold with microporous surface features.	109
Polybutylene terephthalate	The inverse trabecular inner structure from a native canine bone tissue was fabricated by SLA. Intensive bone growth *in vivo* compared with random porous design of scaffolds.	110
Collagen/hyaluronic acid hydrogel	Zonal micropatterning in a bulk hydrogel with 500 μm thickness.	112
PEO gel	Cell encapsulation in a PEO gel using SLA. Encapsulated CHO cells were viable on day 2.	113
PEG–DA	Chondrogenic differentiation of MSCs encapsulated in PEG–DMA gel.	114
PEG–DMA	Viable human fibroblast encapsulated in PEG–DMA gel.	115
	Spatial control of multiple materials including RGD ligands and fluorescently labeled microparticles by SLA.	116, 117
HA	Using a negative epoxy mold fabricated by SLA.	121
	In vitro proliferation of bone marrow stromal cells and mineralized bone tissue formation were observed.	98
	Composite fabrication with photocurable acrylate resin.	120, 121

Poly(propylene fumarate)

PPF is one of the most studied biodegradable and photocrosslinkable polymers.[38,76] With the aid of a photoinitiator, bis(2,4,6,-trimethylbenzoyl) phenylphosphine oxide, PPF chains can be crosslinked into networks. Because of the controllability of PPF photocrosslinking characteristics and mechanical properties as well as the suitable mechanical strength of UV-crosslinked PPF networks,[76] a mixture of PPF and DEF has been investigated for use as an SLA resin material. DEF is added as a solvent to reduce the viscosity, an important criterion for a device with moving part. This has allowed the control of pore size as well as channel and wall thickness features in the 100 μm range.[101–105] Using a commercially available laser curing device, an SLA 250/40 (3D Systems), the first tissue engineering study to fabricate PPF scaffolds with controlled geometry designed using CAD software was published in 2003.[101] An example of a CAD file prior to SLA scaffold fabrication is shown in Figure 2. Figure 3 shows scanning electron microscope (SEM) images of the morphology of controlled architecture 3D PPF/DEF scaffolds with continuous channels, which were fabricated by a 3D systems Viper HA. In addition, it has been shown that a PPF/DEF mixture could be applicable to both SLA[103,104] and other SFF methods such as 3D printing and injection molding.[105] Recent work has demonstrated the feasibility of surface modification of scaffolds by soaking them in a concentrated inorganic ion solution.[102] Moreover, controlling the degradability by varying the molecular weight of PPF

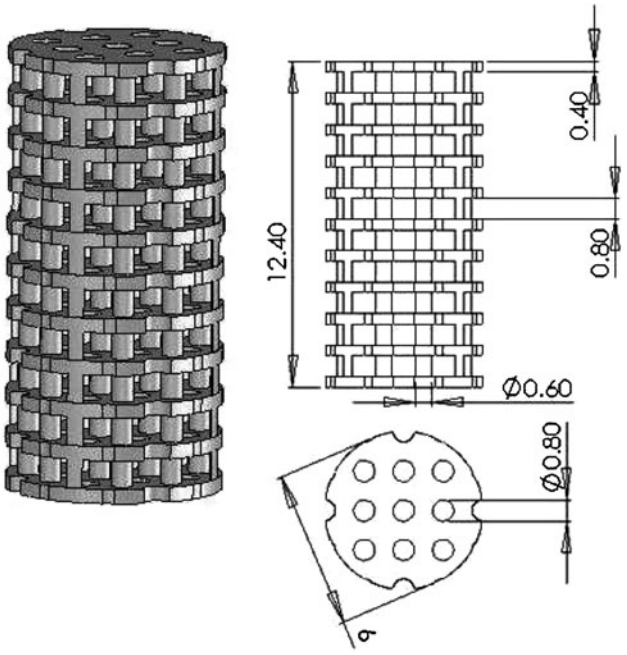

FIG. 2. An example of a computer-aided design file used for SLA scaffold fabrication. We refer to this geometry as the "Plate and Post" scaffold architecture. Dimensions of total length, plate thickness, gap between plates, post diameter, and pore diameter are in millimeters.

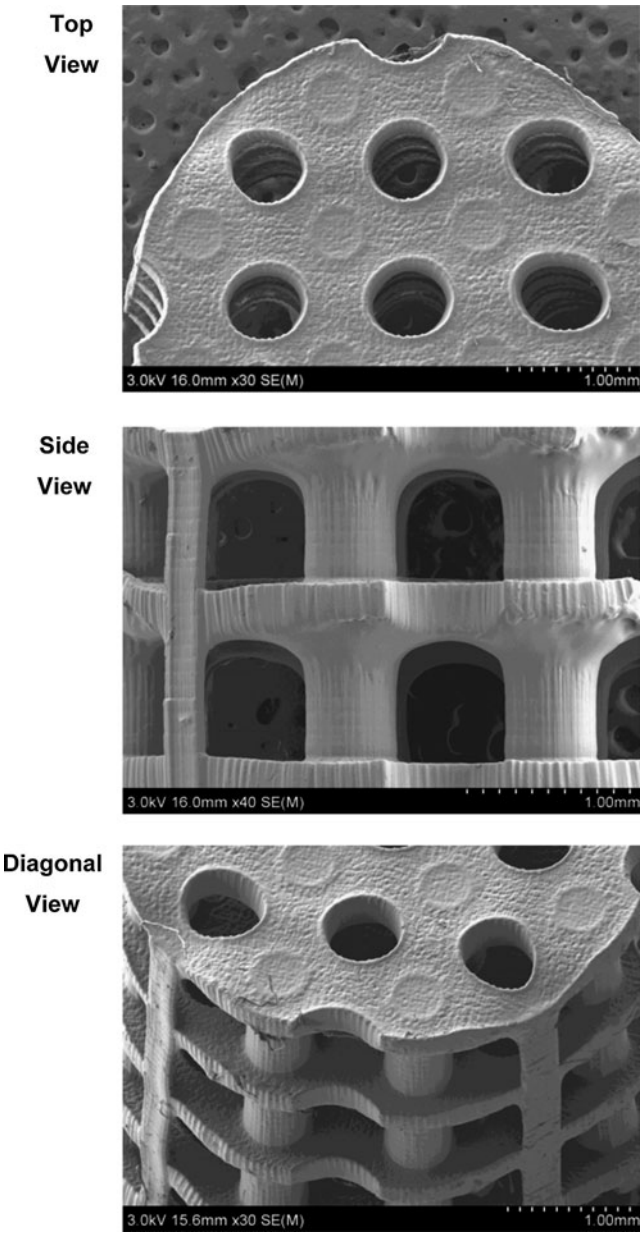

FIG. 3. Scanning electron microscope images of SLA-fabricated poly(propylene fumarate)/diethyl fumarate scaffolds. These images illustrate the interconnected channel geometry of the plate and post scaffold architecture shown in Figure 2.

during the synthesis could be a clinical advantage facilitating neobone development and complete resorption of implanted scaffolds.[106] Given this controllable degradability, PPF polymer with a low number average molecular weight (<800 Da) has been researched.[106]

Other polymeric scaffolds fabricated by SLA

A series of recent studies investigated the fabrication of scaffolds with controlled geometry using several types of resin materials, and *in vitro* cell attachment was assessed. Fumaric acid monoethyl ester functionalized with poly(D,L-lactide) oligomers has been used to create a gyroid architecture.[107] *N*-Vinyl-2-pyrrolodone was used as the accelerator and Lucirin TPO-L was used as the photoinitiator. Initial *in vitro* data demonstrated that mouse preosteoblasts could adhere and spread on this scaffold. Another gyroid scaffold fabricated with poly(D,L-lactide) has also exhibited M3TC3 cell adhesion on day 1.[108] SLA fabrication might also allow control of surface features of 3D porous scaffolds to provide a favorable environment for bone tissue formation.[109] Nanofibrous poly(L-lactic acid) scaffolds have been developed with a micropore structure in the struts that mimics the morphological function of type I collagen and significantly increased surface area compared with a solid-walled scaffold. These nanofibrous scaffolds with rectangular channels were created by using an SLA-fabricated negative mold and thermal phase separation of poly(L-lactic acid) solution. Interestingly, mRNA expression levels of OC and BSP of MC3T3-E1 cells in fibrous scaffolds were higher than solid-walled scaffolds after 2 and 6 weeks of culture. Further, one recent study has revealed the critical importance of 3D porous scaffold structural cues to induce *in vivo* bone regeneration.[110] In addition to the importance of the design and fabrication of accurate morphology of implantable bone substitutes,[111] it is also essential that the internal geometry closely mimics the native bone tissue to induce bone ingrowth. The inverse trabecular inner architecture of SLA-fabricated polybutylene terephthalate scaffolds designed from micro-CT scans of a native cadaveric canine femur exhibited up to six times higher bone growth into and adjacent to the scaffolds, compared with simple porous scaffolds.[111] This study emphasized that macroscopic structural characteristic, specifically inner pore architecture, might facilitate accelerated bone regeneration, specifically inner pore architecture.

Photopolymerized hydrogels

In addition to controlled design of macroporous scaffolds, SLA can be applied to photopolymerized hydrogel systems. For example, 2D patterning on bilayer films has been achieved via soft-photolithography stamping, and micropatterning of interpenetrating polymeric network within 3D hydrogels of collagen and hyaluronic acid was also investigated. This technique may allow the zonal differential distribution of several scaffold properties within a bulk hydrogel, including crosslinking density, swelling degree, water content, and mechanical stiffness.[112]

Cell encapsulation within a photopolymerized hydrogel has also been developed. 3D poly(ethylene oxide) hydrogel encapsulating Chinese hamster ovary cells were fabricated using a commercially available SLA process. This hydrogel system exhibited elastic mechanical property similar to soft tissues, along with high viability of the encapsulated cells on day 2.[113] PEG can be crosslinked into a hydrogel by the incorporation of acrylate or methacrylate as photoreactive and crosslinkable groups. Photoencapsulated MSCs in PEG–DA hydrogel exhibited chondrogenic differentiation for 6 weeks,[114] and encapsulation of human dermal fibroblasts in PEG–dimethacrylate (PEG–DMA) hydrogel could be also accomplished with SLA.[115] Further, this method can be applied to functionalization of the PEG hydrogel with arginine-glycine-aspartic acid ligands for specific localization of cells.[116] These studies have shown the possibility of

multimaterial spatial control using SLA. Therefore, an SLA-fabricated hydrogel containing an encapsulated cell population may be a promising technique for providing sufficient cell mass for large constructs. Moreover, Mapili *et al.* have demonstrated spatiotemporal incorporation of a variety of materials within 3D PEG–DMA scaffolds fabricated by SLA.[117] Fluorescently labeled polymer microparticles such as fluorescein isothiocyanate (FITC)- or Cy5-labeled latex particles were spatially patterned in the scaffold layers. Fibronectin-derived peptides and heparin sulfate have also been successfully conjugated in the scaffold material. This result illustrated the capability of SLA for the accurate distribution of multiple factors such as growth factors within the scaffolds by point-by-point photopolymerization, resulting in a hybrid tissue structure.

HA materials

HA is one of the most intensively researched bioceramics in bone tissue engineering because of its biocompatibility as well as physical and chemical similarity to the inorganic compound in the native bone tissue.[118] Although SLA has been traditionally applied to synthetic polymeric resins to create 3D complex architectures, recent studies have demonstrated the feasibility of controlled HA scaffold design. The direct photopolymerization of polymeric resin results in simultaneous scaffold fabrication, whereas HA scaffolds with controlled architecture are usually fabricated from a negative mold prepared via SLA as well as the casting and subsequent curing of a suspension containing HA, dispersant, monomers, and initiators.[119] Goat bone marrow stromal cells seeded onto the HA scaffold fabricated by this technique showed *in vitro* proliferation on the exterior surface of these scaffolds over 7 days, and methylene blue/basic fuchsin-stained histology data indicated that the mineralized bone tissue was observed after 6 weeks of subcutaneous implantation in athymic nude mice.[98] Another *in vivo* study using designed HA scaffolds in a minipig model demonstrated that the overall shape of regenerated bone tissue may depend on the architecture of scaffold's internal channel geometry.[25]

Further, HA could be used in composite fabrication with photocurable acrylate resins.[120,121] In these studies, micrometer-sized HA particles were incorporated with olygocarbonate dimethacrylate resin material, and simple stirring created homogenous mixture of HA particles and resin polymers, which blocked the inhibition of photocrosslinking by solid particles. Although increasing the amount of HA particles might limit the versatility of SLA fabrication because of increased viscosity, the result of 4- and 8-week *in vivo* studies on distal epiphysis implants in rat femora exhibited extensive periosteal and endosteal osteogenesis, as observed by scanning electron microscopy of sectioned tissue samples.[121] In addition, cell attachment measured by propidium iodide staining and proliferation assessed by DNA contents showed higher levels in composite scaffolds than in the control olygocarbonate dimethacrylate scaffold.[120] Similarly, bioactive glass has also been used for the fabrication of CAD scaffolds with the aid of the combined methods of both SLA and gel casting.[122] An SLA-produced epoxy resin negative mold with controlled architectures was used to cast a homogeneous suspension of a glass slurry. This material was then cast in this mold. It has been hypothesized that bioactive glass material is biocompatible like HA,[123] could control osteogenic differentiation, and could bring about osteogenic gene expression.[124–126] These indirect fabrication techniques using an SLA-fabricated mold and ceramic suspension have shown the versatility of controlled architecture manufacturing and its application in animal models.

Clinical Approaches Utilizing SLA

Since 1987, 3D CT scans of the skull have been used for maxillofacial preoperative planning.[127] Indeed, SLA-derived models have become widely used in the preparation of surgical guides or for planning the manipulation of boney and/or soft tissue structures.[128] More recently, CAD techniques have been used to model[129–131] the performance of inert[111] and tissue-engineered implant models that are to be produced via SFF techniques.

Limitations

The clinical application of SLA-fabricated scaffolds involve several critical steps, including (1) scaffold manufacturing based on 3D CT images, (2) virtual surgical procedure simulation and validation, and (3) the final surgical procedure of implantation.[90,91,127,132] Specifically, the first step of scaffold fabrication using SLA includes data acquisition from CT images of the defect site of patients, virtual model reconstruction using computer software, physical 3D scaffold manufacturing using SLA, and 3D model validation. Therefore, for the successful manufacturing of 3D SLA scaffold architectures, close cooperation of surgeons and tissue engineers is of critical importance. However, research into SLA scaffolds remains limited to fabrication itself and simple *in vitro* (cell attachment) or *in vivo* (animal trial) studies, rather than successful surgical implantation into defect sites in human clinical trials. Moreover, a variety of technical limitations remain unsolved.[133,134] During the step of image acquisition, CT data import error may occur when determining the pixel size and slice thickness, and numerical errors in this step may lead to incorrect virtual reconstruction. Moreover, other drawbacks on obtaining CT data from the patient are also reported, such as inhibition of metal or other implant material on the patient's body because of the signal intervention and patient's movement during the CT scan. In addition, during the step of scaffold manufacturing, model stair-step artifact and irregular surface feature may also be found.[134,135] Further, the degree of skin contractures can become an issue for surgical procedures.[91,133] As obtaining the accuracy of both external implant surface geometry is critical for fitting the implant into the defect sites and the inner pore architecture of a 3D scaffold is related to promoting host tissue ingrowth, the technical difficulties related to scaffold fabrication will need to be addressed in the future. Because of these complex limitations as well as the limited numbers of clinically available biomaterials for the implantable scaffold fabrication, the number of reports about surgical implantation using SLA-manufactured scaffold is few. Clinical use of SLA is currently restricted to models based on CT images of a patient's defect for guidance and planning of surgery, which is beneficial on preoperative evaluation.[136–138]

The Current Clinical Use of Computer-Aided Design for Bone Implants

Dean *et al.* presented CAD of cranial implants[90] and the CAD models that were rendered using SFF were then recast in implantable materials, such as poly(methyl methacrylate)[91,135] or titanium. The milling of titanium (inert) prosthetic cranial plates has been demonstrated[139–141] and the performance of these implants and standard of care procedures were compared.[142] In addition, the level of postoperative complications in patients receiving custom cranial implants following decompressive craniectomies was also considered.[143] Research into the use of CAD for hip or knee implants has also been completed. The advantages of patient-specific knee implants was discussed; however, the expense may prevent access to these implants.[144] It was suggested that custom hip implants were useful for patients with distorted anatomy,[145] but the benefit of patient-specific hip implants was also questioned elsewhere.[146] Moreover, the advantages of custom patellofemoral implants were found and it was predicted that this work will shift toward the use of resorbable materials.[147,148] The use of CAD for cervical spine drill guides and resorbable, patient-specific plating has also been studied.[149,150]

Summary

In bone tissue engineering, a series of structural cues including pore size, porosity, interconnectivity, and stiffness have been found to be critical factors in activating osteogenic signal expression. Successful manipulation and fabrication of controlled architecture with optimal conditions of construction parameters may stimulate osteogenic signal expression as well as subsequent osteogenic differentiation. To this end, SLA is a promising and feasible strategy for fabrication of a designed architecture, which may show the best performance *in vitro* and *in vivo*. Recently developed SLA-manufactured 3D scaffold systems have shown the possibility of clinical implantation. Therefore, controlling the structural parameters may promise successful integration of the implants into the surgical sites and enhancement of bone regeneration. Despite some limitations of a sequential procedure of the scaffold fabrication by SLA and the surgical implantation into humans, development in scaffold construction parameters and SLA fabrication is a promising means for the fabrication of functional bone tissue-engineered substrates. These constructs facilitate osteogenic signal expressions and subsequent osteogenic differentiation of either scaffolds preloaded with cells or scaffold-recruited cells from surrounding tissues. Therefore, it is suggested that the following research should be completed to enable successful clinical implementation of implants manufactured via SLA:

1. Scaffold parameters: extensive investigation optimizing the individual scaffold design parameters and subsequent studies to find synergistic versus negative effects of a combination of individual parameters.
2. Bulk material production: continued development of human implantable (FDA-approved) biomaterials and investigation of composite materials.[151]
3. Tuned SLA fabrication: Achievement of a higher precision of SLA to control the specific range (less than tens of micrometer level) of scaffold architecture, validation of accuracy of CAD scaffolds, and feasible reproduction of the scaffolds.
4. Successful data acquisition from human patients: data acquisition using clinical visualization techniques and the transfer of this data to 3D images to reflect defect sites with higher resolution and minimal error.
5. Clinical applications: more intensive case studies to accrue clinical information and to direct treatment.

Acknowledgments

This work was supported by the National Institutes of Health (R01-DE013740) and the National Science Foundation (CBET 0448684). The authors thank Jonathan Wallace (Graduate Research Assistant, Department of Biomedical Engineering, Case Western Reserve University, Cleveland, OH) for SLA fabrication of PPF/DEF scaffolds and his assistance with Figure 2.

Disclosure Statement

No competing financial interests exist.

References

1. Tare, R.S., Babister, J.C., Kanczler, J., and Oreffo, R.O. Skeletal stem cells: phenotype, biology and environmental niches informing tissue regeneration. Mol Cell Endocrinol **288,** 11, 2008.
2. Bessa, P.C., Casal, M., and Reis, R.L. Bone morphogenetic proteins in tissue engineering: the road from laboratory to clinic, part II (BMP delivery). J Tissue Eng Regen Med **2,** 81, 2008.
3. Bessa, P.C., Casal, M., and Reis, R.L. Bone morphogenetic proteins in tissue engineering: the road from the laboratory to the clinic, part I (basic concepts). J Tissue Eng Regen Med **2,** 1, 2008.
4. Ryoo, H.M., Lee, M.H., and Kim, Y.J. Critical molecular switches involved in BMP-2-induced osteogenic differentiation of mesenchymal cells. Gene **366,** 51, 2006.
5. Senta, H., Park, H., Bergeron, E., Drevelle, O., Fong, D., Leblanc, E., Cabana, F., Roux, S., Grenier, G., and Faucheux, N. Cell responses to bone morphogenetic proteins and peptides derived from them: biomedical applications and limitations. Cytokine Growth Factor Rev **20,** 213, 2009.
6. Maegawa, N., Kawamura, K., Hirose, M., Yajima, H., Takakura, Y., and Ohgushi, H. Enhancement of osteoblastic differentiation of mesenchymal stromal cells cultured by selective combination of bone morphogenetic protein-2 (BMP-2) and fibroblast growth factor-2 (FGF-2). J Tissue Eng Regen Med **1,** 306, 2007.
7. Ng, F., Boucher, S., Koh, S., Sastry, K.S., Chase, L., Lakshmipathy, U., Choong, C., Yang, Z., Vemuri, M.C., Rao, M.S., and Tanavde, V. PDGF, TGF-beta, and FGF signaling is important for differentiation and growth of mesenchymal stem cells (MSCs): transcriptional profiling can identify markers and signaling pathways important in differentiation of MSCs into adipogenic, chondrogenic, and osteogenic lineages. Blood **112,** 295, 2008.
8. Dean, D., Wolfe, M.S., Ahmad, Y., Totonchi, A., Chen, J.E., Fisher, J.P., Cooke, M.N., Rimnac, C.M., Lennon, D.P., Caplan, A.I., Topham, N.S., and Mikos, A.G. Effect of transforming growth factor beta 2 on marrow-infused foam

poly(propylene fumarate) tissue-engineered constructs for the repair of critical-size cranial defects in rabbits. Tissue Eng **11,** 923, 2005.
9. Iwata, J., Hosokawa, R., Sanchez-Lara, P.A., Urata, M., Slavkin, H., and Chai, Y. Transforming growth factor-beta regulates basal transcriptional regulatory machinery to control cell proliferation and differentiation in cranial neural crest-derived osteoprogenitor cells. J Biol Chem **285,** 4975, 2010.
10. Kanczler, J.M., Ginty, P.J., Barry, J.J., Clarke, N.M., Howdle, S.M., Shakesheff, K.M., and Oreffo, R.O. The effect of mesenchymal populations and vascular endothelial growth factor delivered from biodegradable polymer scaffolds on bone formation. Biomaterials **29,** 1892, 2008.
11. Kanczler, J.M., Ginty, P.J., White, L., Clarke, N.M., Howdle, S.M., Shakesheff, K.M., and Oreffo, R.O. The effect of the delivery of vascular endothelial growth factor and bone morphogenic protein-2 to osteoprogenitor cell populations on bone formation. Biomaterials **31,** 1242, 2010.
12. Karner, E., Backesjo, C.M., Cedervall, J., Sugars, R.V., Ahrlund-Richter, L., and Wendel, M. Dynamics of gene expression during bone matrix formation in osteogenic cultures derived from human embryonic stem cells *in vitro*. Biochim Biophys Acta **1790,** 110, 2009.
13. Hollinger, J.O., Hart, C.E., Hirsch, S.N., Lynch, S., and Friedlaender, G.E. Recombinant human platelet-derived growth factor: biology and clinical applications. J Bone Joint Surg Am **90 Suppl 1,** 48, 2008.
14. Patel, M., Dunn, T.A., Tostanoski, S., and Fisher, J.P. Cyclic acetal hydroxyapatite composites and endogenous osteogenic gene expression of rat marrow stromal cells. J Tissue Eng Regen Med. (In press).
15. Salgado, A.J., Coutinho, O.P., and Reis, R.L. Bone tissue engineering: state of the art and future trends. Macromol Biosci **4,** 743, 2004.
16. Khatiwala, C.B., Kim, P.D., Peyton, S.R., and Putnam, A.J. ECM compliance regulates osteogenesis by influencing MAPK signaling downstream of RhoA and ROCK. J Bone Miner Res **24,** 886, 2009.
17. Ling, L., Nurcombe, V., and Cool, S.M. Wnt signaling controls the fate of mesenchymal stem cells. Gene **433,** 1, 2009.
18. Franceschi, R.T., and Xiao, G. Regulation of the osteoblast-specific transcription factor, Runx2: responsiveness to multiple signal transduction pathways. J Cell Biochem **88,** 446, 2003.
19. Teplyuk, N.M., Haupt, L.M., Ling, L., Dombrowski, C., Mun, F.K., Nathan, S.S., Lian, J.B., Stein, J.L., Stein, G.S., Cool, S.M., and van Wijnen, A.J. The osteogenic transcription factor Runx2 regulates components of the fibroblast growth factor/proteoglycan signaling axis in osteoblasts. J Cell Biochem **107,** 144, 2009.
20. Robling, A.G., Castillo, A.B., and Turner, C.H. Biomechanical and molecular regulation of bone remodeling. Annu Rev Biomed Eng **8,** 455, 2006.
21. Kasten, P., Beyen, I., Niemeyer, P., Luginbuhl, R., Bohner, M., and Richter, W. Porosity and pore size of beta-tricalcium phosphate scaffold can influence protein production and osteogenic differentiation of human mesenchymal stem cells: an *in vitro* and *in vivo* study. Acta Biomater **4,** 1904, 2008.
22. Khatiwala, C.B., Peyton, S.R., and Putnam, A.J. Intrinsic mechanical properties of the extracellular matrix affect the behavior of pre-osteoblastic MC3T3-E1 cells. Am J Physiol Cell Physiol **290,** C1640, 2006.
23. Mygind, T., Stiehler, M., Baatrup, A., Li, H., Zoua, X., Flyvbjerg, A., Kassem, M., and Bunger, C. Mesenchymal stem cell ingrowth and differentiation on coralline hydroxyapatite scaffolds. Biomaterials **28,** 1036, 2007.
24. Roy, T.D., Simon, J.L., Ricci, J.L., Rekow, E.D., Thompson, V.P., and Parsons, J.R. Performance of hydroxyapatite bone repair scaffolds created via three-dimensional fabrication techniques. J Biomed Mater Res Part A **67A,** 1228, 2003.
25. Chu, T.M., Orton, D.G., Hollister, S.J., Feinberg, S.E., and Halloran, J.W. Mechanical and *in vivo* performance of hydroxyapatite implants with controlled architectures. Biomaterials **23,** 1283, 2002.
26. Gauthier, O., Bouler, J.M., Aguado, E., Pilet, P., and Daculsi, G. Macroporous biphasic calcium phosphate ceramics: influence of macropore diameter and macroporosity percentage on bone ingrowth. Biomaterials **19,** 133, 1998.
27. Oh, S.H., Park, I.K., Kim, J.M., and Lee, J.H. *In vitro* and *in vivo* characteristics of PCL scaffolds with pore size gradient fabricated by a centrifugation method. Biomaterials **28,** 1664, 2007.
28. Roy, T.D., Simon, J.L., Ricci, J.L., Rekow, E.D., Thompson, V.P., and Parsons, J.R. Performance of degradable composite bone repair products made via three-dimensional fabrication techniques. Journal of Biomedical Materials Research Part A **66A,** 283, 2003.
29. Hollister, S.J. Porous scaffold design for tissue engineering. Nat Mater **4,** 518, 2005.
30. Leong, K.F., Cheah, C.M., and Chua, C.K. Solid freeform fabrication of three-dimensional scaffolds for engineering replacement tissues and organs. Biomaterials **24,** 2363, 2003.
31. Yeatts, A.B., and Fisher, J.P. Biological implications of polymeric scaffolds for bone tissue engineering developed via solid freeform fabrication. In: Khang, G., ed. Handbook of Intelligent Scaffolds for Regenerative Medicine. Singapore: Pan Stanford Publishing. (In press).
32. Bartolo, P.J., Almeida, H.A., Rezende, R.A., Laoui, T., and Bidanda, B. Advanced processes to fabricate scaffolds for tissue engineering. In: Bidanda, B., and Bartolo, P.J., eds. Virtual Prototyping and Bio Manufacturing in Medical Applications. New York: Springer, 2008, pp. 149–170.
33. Hutmacher, D.W., Sittinger, M., and Risbud, M.V. Scaffold-based tissue engineering: rationale for computer-aided design and solid free-form fabrication systems. Trends Biotechnol **22,** 354, 2004.
34. Pham, D.T., and Gault, R.S. A comparison of rapid prototyping technologies. Int J Machine Tools Manufacture **38,** 1257, 1998.
35. Karageorgiou, V., and Kaplan, D. Porosity of 3D biomaterial scaffolds and osteogenesis. Biomaterials **26,** 5474, 2005.
36. Mistry, A.S., and Mikos, A.G. Tissue engineering strategies for bone regeneration. Adv Biochem Eng Biotechnol **94,** 1, 2005.
37. Murphy, C.M., Haugh, M.G., and O'Brien, F.J. The effect of mean pore size on cell attachment, proliferation and migration in collagen-glycosaminoglycan scaffolds for bone tissue engineering. Biomaterials **31,** 461, 2010.
38. Kim, K., Dean, D., Mikos, A.G., and Fisher, J.P. Effect of initial cell seeding density on early osteogenic signal expression of rat bone marrow stromal cells cultured on cross-linked poly(propylene fumarate) disks. Biomacromolecules **10,** 1810, 2009.
39. Hollister, S.J., Maddox, R.D., and Taboas, J.M. Optimal design and fabrication of scaffolds to mimic tissue

properties and satisfy biological constraints. Biomaterials **23,** 4095, 2002.
40. Klenke, F.M., Liu, Y., Yuan, H., Hunziker, E.B., Siebenrock, K.A., and Hofstetter, W. Impact of pore size on the vascularization and osseointegration of ceramic bone substitutes *in vivo*. J Biomed Mater Res A **85,** 777, 2008.
41. Byrne, E.M., Farrell, E., McMahon, L.A., Haugh, M.G., O'Brien, F.J., Campbell, V.A., Prendergast, P.J., and O'Connell, B.C. Gene expression by marrow stromal cells in a porous collagen-glycosaminoglycan scaffold is affected by pore size and mechanical stimulation. J Mater Sci Mater Med **19,** 3455, 2008.
42. Kasten, P., Beyen, I., Niemeyer, P., Luginbuhl, R., Bohner, M., and Richter, W. Porosity and pore size of beta-tricalcium phosphate scaffold can influence protein production and osteogenic differentiation of human mesenchymal stem cells: an in vitro and *in vivo* study. Acta Biomater **4,** 1904, 2008.
43. Karageorgiou, V., and Kaplan, D. Porosity of 3D biornaterial scaffolds and osteogenesis. Biomaterials **26,** 5474, 2005.
44. Sundelacruz, S., and Kaplan, D.L. Stem cell- and scaffold-based tissue engineering approaches to osteochondral regenerative medicine. Semin Cell Dev Biol **20,** 646, 2009.
45. Betz, M.W., Yeatts, A.B., Richbourg, W., Caccamese, J.F., Coletti, D.P., Falco, E.E., and Fisher, J.P. Macroporous hydrogels upregulate osteogenic signal expression and promote bone regeneration. Biomacromolecules 2010 (In press).
46. Alsberg, E., Hill, E.E., and Mooney, D.J. Craniofacial tissue engineering. Crit Rev Oral Biol Med **12,** 64, 2001.
47. Yang, S.F., Leong, K.F., Du, Z.H., and Chua, C.K. The design of scaffolds for use in tissue engineering. Part 1. Traditional factors. Tissue Eng **7,** 679, 2001.
48. Klawitter, J.J., and Hulbert, S.F. Application of porous ceramics for the attachment of load bearing internal orthopedic applications. J Biomed Mater Res Biomed Mater Symp **2,** 161, 1972.
49. Aronin, C.E.P., Sadik, K.W., Lay, A.L., Rion, D.B., Tholpady, S.S., Ogle, R.C., and Botchwey, E.A. Comparative effects of scaffold pore size, pore volume, and total void volume on cranial bone healing patterns using microsphere-based scaffolds. J Biomed Mater Res Part A **89A,** 632, 2009.
50. Roosa, S.M.M., Kemppainen, J.M., Moffitt, E.N., Krebsbach, P.H., and Hollister, S.J. The pore size of polycaprolactone scaffolds has limited influence on bone regeneration in an *in vivo* model. J Biomed Mater Res Part A **92A,** 359, 2010.
51. Volkmer, E., Drosse, I., Otto, S., Stangelmayer, A., Stengele, M., Kallukalam, B.C., Mutschler, W., and Schieker, M. Hypoxia in static and dynamic 3D culture systems for tissue engineering of bone. Tissue Eng Part A **14,** 1331, 2008.
52. Jin, Q.M., Takita, H., Kohgo, T., Atsumi, K., Itoh, H., and Kuboki, Y. Effects of geometry of hydroxyapatite as a cell substratum in BMP-induced ectopic bone formation. J Biomed Mater Res **51,** 491, 2000.
53. Kuboki, Y., Jin, Q.M., and Takita, H. Geometry of carriers controlling phenotypic expression in BMP-induced osteogenesis and chondrogenesis. J Bone Joint Surg Am **83A,** S105, 2001.
54. Uebersax, L., Hagenmuller, H., Hofmann, S., Gruenblatt, E., Muller, R., Vunjak-Novakovic, G., Kaplan, D.L., Merkle, H.P., and Meinel, L. Effect of scaffold design on bone morphology *in vitro*. Tissue Eng **12,** 3417, 2006.
55. Rose, F.R., Cyster, L.A., Grant, D.M., Scotchford, C.A., Howdle, S.M., and Shakesheff, K.M. *In vitro* assessment of cell penetration into porous hydroxyapatite scaffolds with a central aligned channel. Biomaterials **25,** 5507, 2004.
56. Shor, L., Guceri, S., Wen, X., Gandhi, M., and Sun, W. Fabrication of three-dimensional polycaprolactone/hydroxyapatite tissue scaffolds and osteoblast-scaffold interactions *in vitro*. Biomaterials **28,** 5291, 2007.
57. Pamula, E., Filova, E., Bacakova, L., Lisa, V., and Adamczyk, D. Resorbable polymeric scaffolds for bone tissue engineering: the influence of their microstructure on the growth of human osteoblast-like MG 63 cells. J Biomed Mater Res A **89,** 432, 2009.
58. Zhou, H., Chen, S.B., Peng, J.J., and Wang, C.H. A study of effective diffusivity in porous scaffold by Brownian dynamics simulation. J Colloid Interface Sci **342,** 620, 2010.
59. Lu, J.X., Flautre, B., Anselme, K., Hardouin, P., Gallur, A., Descamps, M., and Thierry, B. Role of interconnections in porous bioceramics on bone recolonization *in vitro* and *in vivo*. J Mater Sci Mater Med **10,** 111, 1999.
60. Jones, A.C., Arns, C.H., Hutmacher, D.W., Milthorpe, B.K., Sheppard, A.P., and Knackstedt, M.A. The correlation of pore morphology, interconnectivity and physical properties of 3D ceramic scaffolds with bone ingrowth. Biomaterials **30,** 1440, 2009.
61. Jones, A.C., Arns, C.H., Sheppard, A.P., Hutmacher, D.W., Milthorpe, B.K., and Knackstedt, M.A. Assessment of bone ingrowth into porous biomaterials using micro-CT. Biomaterials **28,** 2491, 2007.
62. Otsuki, B., Takemoto, M., Fujibayashi, S., Neo, M., Kokubo, T., and Nakamura, T. Pore throat size and connectivity determine bone and tissue ingrowth into porous implants: three-dimensional micro-CT based structural analyses of porous bioactive titanium implants. Biomaterials **27,** 5892, 2006.
63. Chu, T.M.G., Orton, D.G., Hollister, S.J., Feinberg, S.E., and Halloran, J.W. Mechanical and *in vivo* performance of hydroxyapatite implants with controlled architectures. Biomaterials **23,** 1283, 2002.
64. Breuls, R.G., Jiya, T.U., and Smit, T.H. Scaffold stiffness influences cell behavior: opportunities for skeletal tissue engineering. Open Orthop J **2,** 103, 2008.
65. Norman, L.L., Stroka, K., and Aranda-Espinoza, H. Guiding axons in the central nervous system: a tissue engineering approach. Tissue Eng Part B Rev **15,** 291, 2009.
66. Schlunck, G., Han, H., Wecker, T., Kampik, D., Meyer-ter-Vehn, T., and Grehn, F. Substrate rigidity modulates cell matrix interactions and protein expression in human trabecular meshwork cells. Invest Ophthalmol Vis Sci **49,** 262, 2008.
67. Guo, W.H., Frey, M.T., Burnham, N.A., and Wang, Y.L. Substrate rigidity regulates the formation and maintenance of tissues. Biophys J **90,** 2213, 2006.
68. Engler, A.J., Sen, S., Sweeney, H.L., and Discher, D.E. Matrix elasticity directs stem cell lineage specification. Cell **126,** 677, 2006.
69. Khatiwala, C.B., Peyton, S.R., Metzke, M., and Putnam, A.J. The regulation of osteogenesis by ECM rigidity in MC3T3-E1 cells requires MAPK activation. J Cell Physiol **211,** 661, 2007.
70. Evans, N.D., Minelli, C., Gentleman, E., LaPointe, V., Patankar, S.N., Kallivretaki, M., Chen, X., Roberts, C.J., and Stevens, M.M. Substrate stiffness affects early differentia-

tion events in embryonic stem cells. Eur Cell Mater **18,** 1, 2009.
71. Rowlands, A.S., George, P.A., and Cooper-White, J.J. Directing osteogenic and myogenic differentiation of MSCs: interplay of stiffness and adhesive ligand presentation. Am J Physiol Cell Physiol **295,** C1037, 2008.
72. Kundu, A.K., Khatiwala, C.B., and Putnam, A.J. Extracellular matrix remodeling, integrin expression, and downstream signaling pathways influence the osteogenic differentiation of mesenchymal stem cells on poly(lactide-*co*-glycolide) substrates. Tissue Eng Part A **15,** 273, 2009.
73. Peyton, S.R., Kim, P.D., Ghajar, C.M., Seliktar, D., and Putnam, A.J. The effects of matrix stiffness and RhoA on the phenotypic plasticity of smooth muscle cells in a 3-D biosynthetic hydrogel system. Biomaterials **29,** 2597, 2008.
74. McBeath, R., Pirone, D.M., Nelson, C.M., Bhadriraju, K., and Chen, C.S. Cell shape, cytoskeletal tension, and RhoA regulate stem cell lineage commitment. Dev Cell **6,** 483, 2004.
75. Declercq, H.A., Cornelissen, M.J., Gorskiy, T.L., and Schacht, E.H. Osteoblast behaviour on *in situ* photopolymerizable three-dimensional scaffolds based on D, L-lactide, epsilon-caprolactone and trimethylene carbonate. J Mater Sci Mater Med **17,** 113, 2006.
76. Fisher, J.P., Dean, D., and Mikos, A.G. Photocrosslinking characteristics and mechanical properties of diethyl fumarate/poly(propylene fumarate) biomaterials. Biomaterials **23,** 4333, 2002.
77. Takahashi, Y., Yamamoto, M., and Tabata, Y. Osteogenic differentiation of mesenchymal stem cells in biodegradable sponges composed of gelatin and beta-tricalcium phosphate. Biomaterials **26,** 3587, 2005.
78. Kuo, Y.C., Yeh, C.F., and Yang, J.T. Differentiation of bone marrow stromal cells in poly(lactide-*co*-glycolide)/chitosan scaffolds. Biomaterials **30,** 6604, 2009.
79. Norman, J.J., Collins, J.M., Sharma, S., Russell, B., and Desai, T.A. Microstructures in 3D biological gels affect cell proliferation. Tissue Eng Part A **14,** 379, 2008.
80. Collins, J.M., Ayala, P., Desai, T.A., and Russell, B. Three-dimensional culture with stiff microstructures increases proliferation and slows osteogenic differentiation of human mesenchymal stem cells. Small **6,** 355, 2010.
81. dos Santos, E.A., Farina, M., Soares, G.A., and Anselme, K. Chemical and topographical influence of hydroxyapatite and beta-tricalcium phosphate surfaces on human osteoblastic cell behavior. J Biomed Mater Res A **89,** 510, 2009.
82. Neel, E.A., Palmer, G., Knowles, J.C., Salih, V., and Young, A.M. Chemical, modulus and cell attachment studies of reactive calcium phosphate filler-containing fast photocuring, surface-degrading, polymeric bone adhesives. Acta Biomater **6,** 2695, 2010.
83. McCullen, S.D., Zhu, Y., Bernacki, S.H., Narayan, R.J., Pourdeyhimi, B., Gorga, R.E., and Loboa, E.G. Electrospun composite poly(L-lactic acid)/tricalcium phosphate scaffolds induce proliferation and osteogenic differentiation of human adipose-derived stem cells. Biomed Mater **4,** 35002, 2009.
84. Dean, D., Topham, N.S., Meneghetti, S.C., Wolfe, M.S., Jepsen, K., He, S., Chen, J.E., Fisher, J.P., Cooke, M., Rimnac, C., and Mikos, A.G. Poly(propylene fumarate) and poly(DL-lactic-*co*-glycolic acid) as scaffold materials for solid and foam-coated composite tissue-engineered constructs for cranial reconstruction. Tissue Eng **9,** 495, 2003.
85. Dawson, J.I., Wahl, D.A., Lanham, S.A., Kanczler, J.M., Czernuszka, J.T., and Oreffo, R.O. Development of specific collagen scaffolds to support the osteogenic and chondrogenic differentiation of human bone marrow stromal cells. Biomaterials **29,** 3105, 2008.
86. Fernandes, H., Dechering, K., Van Someren, E., Steeghs, I., Apotheker, M., Leusink, A., Bank, R., Janeczek, K., Van Blitterswijk, C., and de Boer, J. The role of collagen crosslinking in differentiation of human mesenchymal stem cells and MC3T3-E1 cells. Tissue Eng Part A **15,** 3857, 2009.
87. Buxton, P.G., Bitar, M., Gellynck, K., Parkar, M., Brown, R.A., Young, A.M., Knowles, J.C., and Nazhat, S.N. Dense collagen matrix accelerates osteogenic differentiation and rescues the apoptotic response to MMP inhibition. Bone **43,** 377, 2008.
88. Tierney, C.M., Haugh, M.G., Liedl, J., Mulcahy, F., Hayes, B., and O'Brien, F.J. The effects of collagen concentration and crosslink density on the biological, structural and mechanical properties of collagen-GAG scaffolds for bone tissue engineering. J Mech Behav Biomed Mater **2,** 202, 2009.
89. Anderson, E.J., and Knothe Tate, M.L. Design of tissue engineering scaffolds as delivery devices for mechanical and mechanically modulated signals. Tissue Eng **13,** 2525, 2007.
90. Dean, D., Min, K.J., and Bond, A. Computer aided design of large-format prefabricated cranial plates. J Craniofac Surg **14,** 819, 2003.
91. Min, K., and Dean, D. Highly accurate CAD tools for cranial implants. In: Ellis, R.E., and Peters, T.M., eds. Medical Image Computing and Computer Assisted Intervention. Heidelberg, Germany: Springer Verlag, 2003, pp. 99–107.
92. Sachlos, E., and Czernuszka, J.T. Making tissue engineering scaffolds work. Review: the application of solid freeform fabrication technology to the production of tissue engineering scaffolds. Eur Cell Mater **5,** 29, 2003.
93. Koegler, W.S., and Griffith, L.G. Osteoblast response to PLGA tissue engineering scaffolds with PEO modified surface chemistries and demonstration of patterned cell response. Biomaterials **25,** 2819, 2004.
94. Hutmacher, D.W., Schantz, T., Zein, I., Ng, K.W., Teoh, S.H., and Tan, K.C. Mechanical properties and cell cultural response of polycaprolactone scaffolds designed and fabricated via fused deposition modeling. J Biomed Mater Res **55,** 203, 2001.
95. Landers, R., and Mulhaupt, R. Desktop manufacturing of complex objects, prototypes and biomedical scaffolds by means of computer-assisted design combined with computer-guided 3D plotting of polymers and reactive oligomers. Macromolecular Materials and Engineering **282,** 17, 2000.
96. Williams, J.M., Adewunmi, A., Schek, R.M., Flanagan, C.L., Krebsbach, P.H., Feinberg, S.E., Hollister, S.J., and Das, S. Bone tissue engineering using polycaprolactone scaffolds fabricated via selective laser sintering. Biomaterials **26,** 4817, 2005.
97. Lin, C.Y., Wirtz, T., LaMarca, F., and Hollister, S.J. Structural and mechanical evaluations of a topology optimized titanium interbody fusion cage fabricated by selective laser melting process. J Biomed Mater Res A **83,** 272, 2007.
98. Wilson, C.E., de Bruijn, J.D., van Blitterswijk, C.A., Verbout, A.J., and Dhert, W.J. Design and fabrication of standardized hydroxyapatite scaffolds with a defined

macro-architecture by rapid prototyping for bone-tissue-engineering research. J Biomed Mater Res A **68,** 123, 2004.
99. Fernandez, J.G., Mills, C.A., Martinez, E., Lopez-Bosque, M.J., Sisquella, X., Errachid, A., and Samitier, J. Micro- and nanostructuring of freestanding, biodegradable, thin sheets of chitosan via soft lithography. J Biomed Mater Res A **85,** 242, 2008.
100. Bhattarai, N., Edmondson, D., Veiseh, O., Matsen, F.A., and Zhang, M. Electrospun chitosan-based nanofibers and their cellular compatibility. Biomaterials **26,** 6176, 2005.
101. Cooke, M.N., Fisher, J.P., Dean, D., Rimnac, C., and Mikos, A.G. Use of stereolithography to manufacture critical-sized 3D biodegradable scaffolds for bone ingrowth. J Biomed Mater Res B Appl Biomater **64,** 65, 2003.
102. Lan, P.X., Lee, J.W., Seol, Y.J., and Cho, D.W. Development of 3D PPF/DEF scaffolds using micro-stereolithography and surface modification. J Mater Sci Mater Med **20,** 271, 2009.
103. Lee, J.W., Lan, P.X., Kim, B., Lim, G., and Cho, D.W. Fabrication and characteristic analysis of a poly(propylene fumarate) scaffold using micro-stereolithography technology. J Biomed Mater Res B Appl Biomater **87,** 1, 2008.
104. Lee, K.W., Wang, S., Fox, B.C., Ritman, E.L., Yaszemski, M.J., and Lu, L. Poly(propylene fumarate) bone tissue engineering scaffold fabrication using stereolithography: effects of resin formulations and laser parameters. Biomacromolecules **8,** 1077, 2007.
105. Lee, K.W., Wang, S., Lu, L., Jabbari, E., Currier, B.L., and Yaszemski, M.J. Fabrication and characterization of poly(propylene fumarate) scaffolds with controlled pore structures using 3-dimensional printing and injection molding. Tissue Eng **12,** 2801, 2006.
106. Dean, D., Wallace, J., Kim, K., Mikos, A.G., and Fisher, J.P. Stereolithographic rendering of low molecular weight polymer scaffolds for bone tissue engineering. In: da Silva Bártolo, P.J., *et al.*, eds. Innovative Developments in Design and Manufacturing: Advanced Research in Virtual and Rapid Prototyping. Boca Raton, FL: CRC Press (Taylor & Francis), 2010, pp. 37–43.
107. Jansen, J., Melchels, F.P., Grijpma, D.W., and Feijen, J. Fumaric acid monoethyl ester-functionalized poly(D, L-lactide)/*N*-vinyl-2-pyrrolidone resins for the preparation of tissue engineering scaffolds by stereolithography. Biomacromolecules **10,** 214, 2009.
108. Melchels, F.P., Feijen, J., and Grijpma, D.W. A poly(D,L-lactide) resin for the preparation of tissue engineering scaffolds by stereolithography. Biomaterials **30,** 3801, 2009.
109. Chen, V.J., Smith, L.A., and Ma, P.X. Bone regeneration on computer-designed nano-fibrous scaffolds. Biomaterials **27,** 3973, 2006.
110. Geffre, C.P., Margolis, D.S., Ruth, J.T., DeYoung, D.W., Tellis, B.C., and Szivek, J.A. A novel biomimetic polymer scaffold design enhances bone ingrowth. J Biomed Mater Res A **91,** 795, 2009.
111. Ciocca, L., De Crescenzio, F., Fantini, M., and Scotti, R. CAD/CAM and rapid prototyped scaffold construction for bone regenerative medicine and surgical transfer of virtual planning: a pilot study. Comput Med Imaging Graph **33,** 58, 2009.
112. Suri, S., and Schmidt, C.E. Photopatterned collagen-hyaluronic acid interpenetrating polymer network hydrogels. Acta Biomater **5,** 2385, 2009.
113. Dhariwala, B., Hunt, E., and Boland, T. Rapid prototyping of tissue-engineering constructs, using photopolymerizable hydrogels and stereolithography. Tissue Eng **10,** 1316, 2004.
114. Williams, C.G., Kim, T.K., Taboas, A., Malik, A., Manson, P., and Elisseeff, J. *In vitro* chondrogenesis of bone marrow-derived mesenchymal stem cells in a photopolymerizing hydrogel. Tissue Eng **9,** 679, 2003.
115. Arcaute, K., Mann, B.K., and Wicker, R.B. Stereolithography of three-dimensional bioactive poly(ethylene glycol) constructs with encapsulated cells. Ann Biomed Eng **34,** 1429, 2006.
116. Arcaute, K., Mann, B., and Wicker, R. Stereolithography of spatially controlled multi-material bioactive poly(ethylene glycol) scaffolds. Acta Biomater **6,** 1047, 2009.
117. Mapili, G., Lu, Y., Chen, S., and Roy, K. Laser-layered microfabrication of spatially patterned functionalized tissue-engineering scaffolds. J Biomed Mater Res B Appl Biomater **75,** 414, 2005.
118. Kim, K., and Fisher, J.P. Nanoparticle technology in bone tissue engineering. J Drug Target **15,** 241, 2007.
119. Chu, T.M., Halloran, J.W., Hollister, S.J., and Feinberg, S.E. Hydroxyapatite implants with designed internal architecture. J Mater Sci Mater Med **12,** 471, 2001.
120. Barry, J.J., Evseev, A.V., Markov, M.A., Upton, C.E., Scotchford, C.A., Popov, V.K., and Howdle, S.M. *In vitro* study of hydroxyapatite-based photocurable polymer composites prepared by laser stereolithography and supercritical fluid extraction. Acta Biomater **4,** 1603, 2008.
121. Popov, V.K., Evseev, A.V., Ivanov, A.L., Roginski, V.V., Volozhin, A.I., and Howdle, S.M. Laser stereolithography and supercritical fluid processing for custom-designed implant fabrication. J Mater Sci Mater Med **15,** 123, 2004.
122. Padilla, S., Sanchez-Salcedo, S., and Vallet-Regi, M. Bioactive glass as precursor of designed-architecture scaffolds for tissue engineering. J Biomed Mater Res A **81,** 224, 2007.
123. Padilla, S., Sanchez-Salcedo, S., and Vallet-Regi, M. Bioactive and biocompatible pieces of HA/sol-gel glass mixtures obtained by the gel-casting method. J Biomed Mater Res A **75,** 63, 2005.
124. Gough, J.E., Jones, J.R., and Hench, L.L. Nodule formation and mineralisation of human primary osteoblasts cultured on a porous bioactive glass scaffold. Biomaterials **25,** 2039, 2004.
125. Jones, J.R., Tsigkou, O., Coates, E.E., Stevens, M.M., Polak, J.M., and Hench, L.L. Extracellular matrix formation and mineralization on a phosphate-free porous bioactive glass scaffold using primary human osteoblast (HOB) cells. Biomaterials **28,** 1653, 2007.
126. Meseguer-Olmo, L., Bernabeu-Esclapez, A., Ros-Martinez, E., Sanchez-Salcedo, S., Padilla, S., Martin, A.I., Vallet-Regi, M., Clavel-Sainz, M., Lopez-Prats, F., and Meseguer-Ortiz, C.L. *In vitro* behaviour of adult mesenchymal stem cells seeded on a bioactive glass ceramic in the SiO(2)-CaO-P(2)O(5) system. Acta Biomater **4,** 1104, 2008.
127. Robiony, M., Salvo, I., Costa, F., Zerman, N., Bazzocchi, M., Toso, F., Bandera, C., Filippi, S., Felice, M., and Politi, M. Virtual reality surgical planning for maxillofacial distraction osteogenesis: the role of reverse engineering rapid prototyping and cooperative work. J Oral Maxillofac Surg **65,** 1198, 2007.
128. D'Urso, P.S., Williamson, O.D., and Thompson, R.G. Biomodeling as an aid to spinal instrumentation. Spine (Phila Pa 1976) **30,** 2841, 2005.

129. Juergens, P., Krol, Z., Zeilhofer, H.F., Beinemann, J., Schicho, K., Ewers, R., and Klug, C. Computer simulation and rapid prototyping for the reconstruction of the mandible. J Oral Maxillofac Surg **67,** 2167, 2009.
130. Kluess, D., Souffrant, R., Mittelmeier, W., Wree, A., Schmitz, K.P., and Bader, R. A convenient approach for finite-element-analyses of orthopaedic implants in bone contact: modeling and experimental validation. Comput Methods Programs Biomed **95,** 23, 2009.
131. Sagbo, S., Blochaou, F., Langlotz, F., Vangenot, C., Nolte, L.P., and Zheng, G. New orthopaedic implant management tool for computer-assisted planning, navigation, and simulation: from implant CAD files to a standardized XML-based implant database. Comput Aided Surg **10,** 311, 2005.
132. Lal, K., White, G.S., Morea, D.N., and Wright, R.F. Use of stereolithographic templates for surgical and prosthodontic implant planning and placement. Part I. The concept. J Prosthodont **15,** 51, 2006.
133. D'Urso, P.S., Earwaker, W.J., Barker, T.M., Redmond, M.J., Thompson, R.G., Effeney, D.J., and Tomlinson, F.H. Custom cranioplasty using stereolithography and acrylic. Br J Plast Surg **53,** 200, 2000.
134. Winder, J., and Bibb, R. Medical rapid prototyping technologies: state of the art and current limitations for application in oral and maxillofacial surgery. J Oral Maxillofac Surg **63,** 1006, 2005.
135. Min, K., and Dean, D. Surface smoothing and template partitioning for cranial implant CAD. In: Galloway, R.L.J., and Cleary, K.R., eds. Medical Imaging 2005: Visualization, Image-Guided Procedures, and Display. Bellingham, WA: SPIE—The International Society for Optical Enginnering, 2005, pp. 492–503.
136. Cohen, A., Laviv, A., Berman, P., Nashef, R., and Abu-Tair, J. Mandibular reconstruction using stereolithographic 3-dimensional printing modeling technology. Oral Surg Oral Med Oral Pathol Oral Radiol Endod **108,** 661, 2009.
137. Holck, D.E., Boyd, E.M., Jr., Ng, J., and Mauffray, R.O. Benefits of stereolithography in orbital reconstruction. Ophthalmology **106,** 1214, 1999.
138. Wagner, J.D., Baack, B., Brown, G.A., and Kelly, J. Rapid 3-dimensional prototyping for surgical repair of maxillofacial fractures: a technical note. J Oral Maxillofac Surg **62,** 898, 2004.
139. Carr, J.C., Fright, W.R., and Beatson, R.K. Surface interpolation with radial basis functions for medical imaging. IEEE Trans Med Imaging **16,** 96, 1997.
140. Eufinger, H., Wehmoller, M., Machtens, E., Heuser, L., Harders, A., and Kruse, D. Reconstruction of craniofacial bone defects with individual alloplastic implants based on CAD/CAM-manipulated CT-data. J Craniomaxillofac Surg **23,** 175, 1995.
141. Scholz, M., Wehmoller, M., Lehmbrock, J., Schmieder, K., Engelhardt, M., Harders, A., and Eufinger, H. Reconstruction of the temporal contour for traumatic tissue loss using a CAD/CAM-prefabricated titanium implant-case report. J Craniomaxillofac Surg **35,** 388, 2007.
142. Lee, S.C., Wu, C.T., Lee, S.T., and Chen, P.J. Cranioplasty using polymethyl methacrylate prostheses. J Clin Neurosci **16,** 56, 2009.
143. Nassiri, N., Cleary, D.R., and Ueeck, B.A. Is cranial reconstruction with a hard-tissue replacement patient-matched implant as safe as previously reported? A 3-year experience and review of the literature. J Oral Maxillofac Surg **67,** 323, 2009.
144. Harrysson, O.L., Hosni, Y.A., and Nayfeh, J.F. Custom-designed orthopedic implants evaluated using finite element analysis of patient-specific computed tomography data: femoral-component case study. BMC Musculoskelet Disord **8,** 91, 2007.
145. Koulouvaris, P., Stafylas, K., Sculco, T., and Xenakis, T. Custom-design implants for severe distorted proximal anatomy of the femur in young adults followed for 4–8 years. Acta Orthop **79,** 203, 2008.
146. Gotze, C., Rosenbaum, D., Hoedemaker, J., Bottner, F., and Steens, W. Is there a need of custom-made prostheses for total hip arthroplasty? Gait analysis, clinical and radiographic analysis of customized femoral components. Arch Orthop Trauma Surg **129,** 267, 2009.
147. Chim, H., and Schantz, J.T. New frontiers in calvarial reconstruction: integrating computer-assisted design and tissue engineering in cranioplasty. Plast Reconstr Surg **116,** 1726, 2005.
148. Sisto, D.J., and Sarin, V.K. Patellofemoral arthroplasty with a customized trochlear prosthesis. Orthop Clin North Am **39,** 355, 2008.
149. Ryken, T.C., Kim, J., Owen, B.D., Christensen, G.E., and Reinhardt, J.M. Engineering patient-specific drill templates and bioabsorbable posterior cervical plates: a feasibility study. J Neurosurg Spine **10,** 129, 2009.
150. Ryken, T.C., Owen, B.D., Christensen, G.E., and Reinhardt, J.M. Image-based drill templates for cervical pedicle screw placement. J Neurosurg Spine **10,** 21, 2009.
151. Lee, M.H., Arcidiacono, J.A., Bilek, A.M., Wille, J.J., Hamill, C.A., Wonnacott, K.M., Wells, M.A., and Oh, S.S. Considerations for tissue-engineered and regenerative medicine product development prior to clinical trials in the United States. Tissue Eng Part B Rev **16,** 41, 2010.
152. Murphy, C.M., Haugh, M.G., and O'Brien, F.J. The effect of mean pore size on cell attachment, proliferation and migration in collagen-glycosaminoglycan scaffolds for bone tissue engineering. Biomaterials **31,** 461, 2003.

Address correspondence to:
John P. Fisher, Ph.D.
Fischell Department of Bioengineering
University of Maryland
3238 Jeong H. Kim Engineering Building (# 225)
College Park, MD 20742

E-mail: jpfisher@umd.edu

Received: March 19, 2010
Accepted: May 21, 2010
Online Publication Date: June 22, 2010